CrossMark

# Study of Multilayer X-ray Absorbers to Improve Detection Efficiency of TES X-ray Microcalorimeter Arrays

**T. Hayashi[1] · K. Nagayoshi[1] · H. Muramatsu[1] ·
N.Y. Yamasaki[1] · K. Mitsuda[1] · M. Saito[2] ·
T. Homma[3] · T. Hara[4] · H. Noda[5]**

**Abstract** We report the fabrication and evaluation of the Cu/Bi bilayer absorber with electrodeposition. We designed the Cu/Bi absorber to satisfy the requirements for scanning transmission electron microscope (STEM). The residual resistivity ratios of films of Cu and Bi with electrodeposition was $5.91 \pm 0.49$ and $2.06 \pm 0.33$, respectively; these values are sufficient for the requirements of STEM. We found that the Cu/Bi bilayer absorber TES microcalorimeter experienced a pulse-shape variation and we considered that these variations were caused by the quality of the contact surface between the absorber and TES. In addition, we examined the structure of the absorber using focus ion beam analysis and STEM. The results suggest that an oxidation between the Cu and seed layer, in which the layer is an electrode for electrodeposition, yielded variations. Moreover, thermal simulation suggests that the thermal conduction between the absorber and TES caused variations. The results of this study will improve the process of Bi electrodeposition.

---

✉ T. Hayashi
tasuku@astro.isas.jaxa.jp

[1] Department of Physics, ISAS/JAXA, 3-1-1, Yoshinodai, Tyuoku, Sagamihara, Kanagawa 252-5210, Japan

[2] Research Organization for Nano & Life Innovation, Waseda University, Tokyo, Japan

[3] Department of Applied Chemistry, Research Organization for Nano & Life Innovation, Waseda University, Tokyo, Japan

[4] NIMS, 1-1, Namiki, Tsukuba, Ibaraki 305-0044, Japan

[5] RIKEN, 2-1, Hirosawa, Wako, Saitama 351-0198, Japan

# 1 Introduction

In microcalorimeters used for astronomical applications, high spatial coverage is essential because the number of photons is limited and invaluable. An example are so-called mushroom-shape absorbers that cover the dead space between pixels. Additionally, we require relatively large ($\sim$0.5 mm$^2$) pixels, as this degrades the energy resolution because of an increase in heat capacity and the pulse shape having X-ray absorption position dependence. Bi is the ideal material due to its low specific heat capacity and high X-ray stopping power. We developed the Bi absorber using vapor deposition, which has low heat conductance, but has a pulse-to-pulse variation of decay time constant [1]. Due to its low heat conductance, the Bi absorber might produce pulse shape variations. Thus, to improve the thermal conductivity, it was used with a high-thermal conductance material such as Cu. Furthermore, we developed the Cu absorber with electrodeposition. We obtained a residual resistivity ratio (RRR) value of 11 with our electrodeposition, which is superior to previous vapor deposition obtained (Nagayoshi et al. [2]). Therefore, we fabricated a bilayer absorber of Bi and Cu using the electrodeposition process.

# 2 Prototype Design

We designed a Cu/Bi absorber on TES for STEM [3,4]. We set the energy resolution to less than 10 eV and the saturation energy to more than 15 keV as our design values, and we adopted an absorber size (120 $\mu$m$^2$) smaller than that of TES in the evaluation of the fabrication process of the Cu/Bi bilayer (Fig. 1). Moreover, we determined the absorber thickness to satisfy the requirements for STEM described by Muramatsu et al. [5]. The Cu absorber takes most of the heat capacity of the TES microcalorimeter. To meet the demand of saturation energy, the required thickness of Cu is 1.0 $\mu$m, while the Bi absorber must be 3.0 $\mu$m thick to satisfy the demand of efficiency (80 % at 6 keV). To meet the requirements, the RRR of Cu must be more than 3 and that of Bi more than 1.
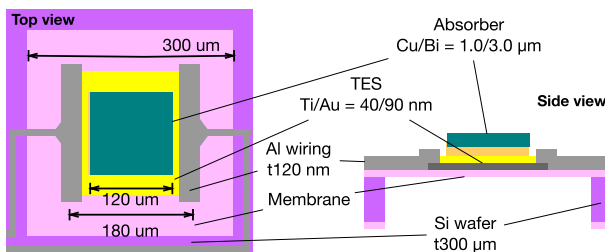


**Fig. 1** *Left* is a schematic drawing of TES design, *Right* is the side view of one pixel TES with absorber (Color figure online)

## 3 Fabrication of Cu/Bi Bilayer Absorber with Electrodeposition

We fabricated the Cu/Bi bilayer absorber using electrodeposition, in the facilities of the Nano Technology Research Center (NTRC) of Waseda University. We controlled the electric potential of the electrodes using potentiostatic electrolysis. To measure the exact current, we used three-electrode-type electrolysis, which involves three electrodes named the working electrode (WE), reference electrode (RE), and counter electrode (CE). The solution temperature was controlled to 40 C by a heater, and the solution was diffused using a stirring bar (Fig. 2). From the results of the cathodal polarization measurements, we determined the electric potential for Bi and Cu deposition to $\sim -50$ and $\sim -400$ mV, the amount of substances to 1 and 10 mmol, and electrodeposition time to 30 and 120 min. The RRR of the films of Cu and Bi were $5.91 \pm 0.49$ and $2.06 \pm 0.33$.

The Cu/Bi absorber TES X-ray microcalorimeter was fabricated in-house with the following process. We use a Si wafer of 300 $\mu$m thick with deposited a $SiO_2$ and a $SiN_x$ by a low-pressure chemical vapor deposition (LPCVD). The thicknesses of the $SiO_2$ and $SiN_x$ are, respectively, 0.5 and 1.0 $\mu$m. Firstly, the $SiN_x$ of the frontside is removed as an alignment mark by reactive ion etching (RIE). The $SiN_x$ and $SiO_2$ of the backside are removed as a membrane pattern by the RIE and the wet etching [5]. The TES is the bilayer of Ti and Au, deposited on $SiN_x$ by DC magnetron sputtering [6]. The Al wiring is created by etching and lift off process (Fig. 3-1). Then, we form an absorber pattern with a photoresist (Fig. 3-2). On the absorber pattern, "seed layer" is deposited by electron beam vapor deposition. The seed layer is bilayer of Ti and Au (Ti/Au = 20/500 nm), which works as an electrode during the processing. The Ti of the seed layer makes adhesion strong between the TES and the Au of seed layer(Fig. 3-3). Then, we again form the absorber pattern of an optimum size for electrodeposition (Fig. 3-4). After the electrodeposition of the bilayer absorber with the above condition, we removed the photoresist and the seed layer (Fig. 3-5–8). Finally, the membrane is etched by deep RIE (DRIE).
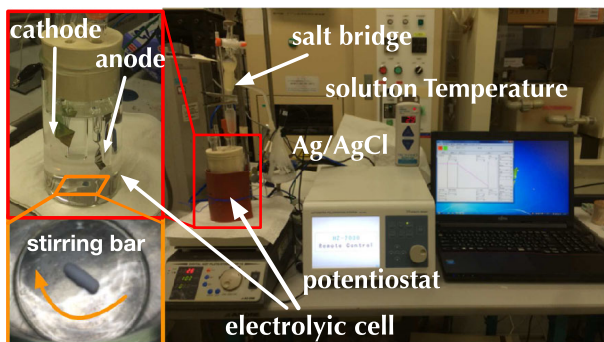


**Fig. 2** The electrodeposition system: The entire electrodeposition system is shown in the *left* picture. A PC controls the current, and the voltage of a potentiostat is located in the center. The solution temperature is monitored by a thermocouple and controlled by a heater. A close-up of the electrolysis cell and stirring bar at the cell's bottom are also shown (Color figure online)
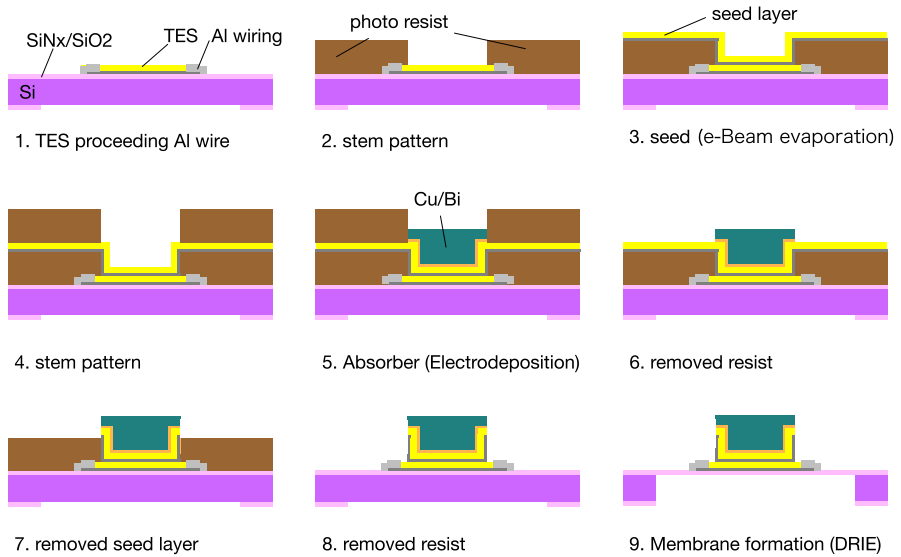
**Fig. 3** Fabrication process of the X-ray microcalorimeter (Color figure online)

## 4 Evaluation

Figure 4-(*left*) shows the completed TES X-ray chip. The thickness of the absorber measured 2 μm, while the designed and processed parameter was 4 μm.
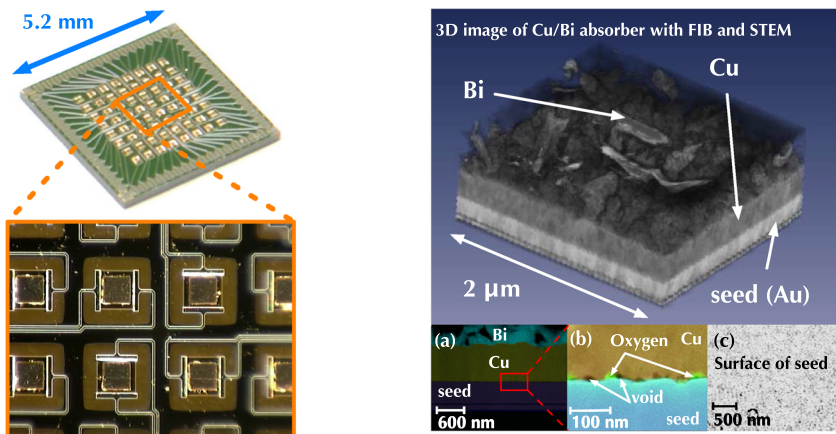


**Fig. 4** *Left* An overview and a close-up view of the Cu/Bi absorber bilayer TES X-ray microcalorimeter array chip. *Right* 3D image of Cu/Bi absorber TES produced using FIB and STEM. **a** is the compositional analysis with EDS, where the top layer is the Bi, second layer is the Cu, and the thread layer is the seed; **b** is an extended image of the red line; and **c** is the boundary surface between Cu and the seed layer, where *black dots* are voids or oxides (Color figure online)

We performed an X-ray irradiation test. We used the dilution refrigerator, which has a lowest temperature of ∼50 mK in ISAS/JAXA, set to the cold stage made from Cu in a dilution refrigerator, and placed the TES chip on this cold stage. $^{55}$Fe isotopes were mounted above the TES chip as X-ray sources. One 64-pixel array TES with a Cu/Bi absorber was voltage biased and lined to SQUID readout.

We measured the TES resistance as a function of temperature at the cold stage. The transition temperature ($T_c$) was ∼300 mK, which differs from our designed value of 200 mK. We do not yet understand the reason for this discrepancy. Furthermore, we measured the $I - V$ property and calculated the resistance ($R \sim 40.3$ mΩ), the transition temperature ($T \sim 289$ mK), the thermal conductance ($G \sim 7.84$ nW/K), the heat capacity ($C \sim 2.14$ pJ/K), and the ($\alpha \sim 70$) at the TES operating point, and then proceeded to measure the X-ray spectrum of the Cu/Bi absorber TES. The bath temperature was set to 230 mK, with a TES bias current of 1110 μA. We obtained an X-ray pulse at this operating point and measured the pulse decay time ($\tau_{\mathrm{eff}} \sim 22$ μs), the energy resolution ($\Delta E_{\mathrm{FWHM}} = 19.67 \pm 1.53$ eV at 5.9 keV), and the base line resolution (13 eV). In addition, we found the pulse-to-pulse variations (∼0.1 μs) of the pulse decay time. We theorized that these variations caused the difference between the energy and base line resolution.

## 5 Microanalysis and Thermal Simulation

To identify the origin of the pulse-to-pulse variation in the decay time constant, we examined the microanalysis of the Cu/Bi absorber. We created a 3D image (Fig. 4-right) of the Cu/Bi absorber using a FIB instrument and scanning electron microscope (SEM), and we performed compositional analysis (Fig. 4-right a) using the STEM. As a result, we found that there were particle variations of Bi (§6) and that there were oxides and voids between the Cu and seed layer; we considered that the oxides and voids between the Cu and seed layer caused the pulse-to-pulse variation. For the construction of the thermal mathematical model to simulate heat diffusion in the TES, we used the finite element method software Thermal Desktop/SINDA. Thermal simulations were performed to identify the origin of the pulse-shape variation. Their details results will be reported in a forthcoming paper. As a result, it may suggest that thermal conductance in the actual TES microcalorimeter array with the multilayer absorber is inhomogeneous, unlike our assumption in our model.

## 6 Improvement of Bi Electrodeposition Method and Conclusion

The particle variations of Bi cause problems in the electrodeposition process. To improve the Bi layer, we revised a part of our process, such as using paddle diffusion instead of the stirring bar and adjusting the current from constant voltage to pulse drive. Paddle diffusion yields superior results to a stirring bar when attempting to address the diffusion limitation of the homogeneity of electron density in solution, while the pulse voltage method inhibits nuclide growth. To confirm these process revisions, we compared the granule size of electrodeposited Bi through electron microscope observation. Figure 5 shows the comparison of the Bi surface before and after the
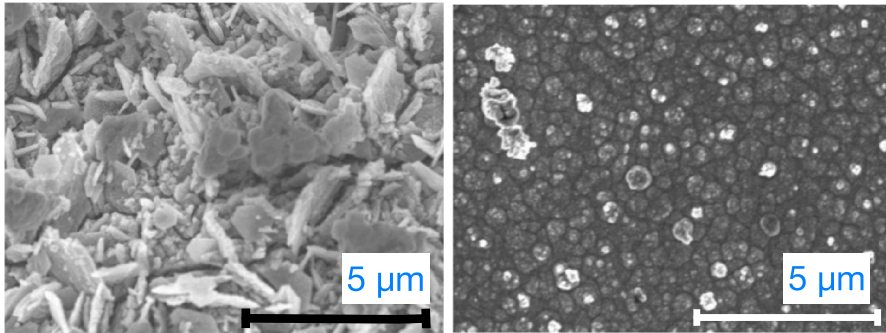
**Fig. 5** SEM image of Bi film. The *Left* figure is Bi before the changing process. The *Right* figure is Bi after the changing process

improvement of the process. It is clear that they become small and round, with a uniform surface.

In summary, we fabricated the Cu/Bi absorber on TES. In operating TES, we confirmed the pulse-to-pulse variation and degradation from the baseline resolution. Thermal model simulation suggests that thermal conductance was inhomogeneous. By using SEM, we confirmed that the Bi particles are rough and inhomogeneous, and, using STEM, we found an oxide film between the Cu and seed layer. Moreover, we found that revising the process improves the inhomogeneity of Bi. Furthermore, we hypothesize that the oxide film is dissolved with the seed layer by using the seed layer of Cu. Therefore, we implemented the fabrication of the Cu/Bi absorber X-ray microcalorimeter TES with high spatial coverage.

# References

1. T. Yoshino, K. Yoshida, T. Hagihara, K. Sato, U. Morita, Y. Ishisaki, R. Fujimoto, N.Y. Yamasaki, K. Mitsuda, Nucl. Instrum. Meth. A. **559**, 432–435 (2006). doi:10.1016/j.nima.2005.12.174
2. K. Nagayoshi et al., Master thesis in University of Tokyo (2012), pp. 45–46
3. K. Maehata, T. Hara, K. Mitsuda, M. Hidaka, K. Tanaka, Y. Yamanaka, J. Low Temp. Phys., in this Special Issue. doi:10.1007/s10909-015-1361-3
4. K. Nagayoshi, T. Hayashi, H. Muramatsu, N. Y. Yamasaki, K. Mitsuda, T. Hara, J. Low Temp. Phys., in this Special Issue
5. H. Muramatsu, K. Nagayoshi, T. Hayashi, K. Sakai, K. Mitsuda, N.Y. Yamasaki, K. Maehata, T. Hara, J. Low Temp. Phys., in this Special Issue. doi:10.1007/s10909-016-1547-3
6. T. Yoshino, K. Mukai, Y. Ezoe, N.Y. Yamasaki, K. Mitsuda, H. Kurabayashi, Y.Ishisaki, T. takano, R. Maeda, J. Low Temp. Phys. **151**, 185–189 (2008). doi:10.1007/s10909-007-9617-1